IEEE Robotics and Automation Letters (RAL) paper presented at the
2020 IEEE/RSJ International Conference on Intelligent Robots and Systems (IROS)
October 25-29, 2020, Las Vegas, NV, USA (Virtual)

Design and Modelling of a Minimally Actuated Serial Robot

Yotam Ayalon, Lior Damti and David Zarrouk

***Abstract*—In this paper we present a minimally actuated overly redundant serial robot (MASR). The robot is composed of a planar arm comprised of ten passive rotational joints and a single mobile actuator that travels over the links to reach designated joints and rotate them. The joints remain locked, using a worm gear setup, after the mobile actuator moves to another link. A gripper is attached to the mobile actuator thus allowing it to transport objects along the links to decrease the actuation of the joints and the working time. A linear stepper motor is used to control the vertical motion of the robot in 3D space. Along the paper, we present the mechanical design of the robot with 10 passive joints and the automatic actuation of the mobile actuator. We also present an optimization algorithm and simulations designed to minimize the working time and the travelled distance of the mobile actuator. Multiple experiments conducted using a robotic prototype depict the advantages of the MASR robot: its very low weight compared to similar robots, its high modularity and the ease of replacement of its parts since there is no wiring along the arm, as shown in the accompanying video.**

***Index Terms*— Serial robot, Minimal actuation, Mobile actuator, Mechanical design.**

I. Introduction

Conventional serial robots are composed of several rigid links connected to each other using actuated joints. Most 3-dimensional commercially available serial robots have between 4 and 7 degrees of freedom. In tasks that call for maneuvering in confined spaces, traditional serial robots are often insufficient. In some industries the inability to do certain tasks because of restricted access has major commercial significance.

The prime reason for developing hyper redundant robots (alternatively known as snake robots), is their ability to navigate around obstacles and in highly confined spaces. They are typically actuated using 10 to 20 motors [1]-[3]. Extensive research over the past several decades has generated many different configurations and mechanisms for a variety of applications such as search and rescue operations [4]-[12], as well as maintenance and medical applications for minimally invasive procedures [13]-[18]. Due to their relatively low weight, these robots [19]-[22] as well as continuum robots [23] are possible candidates for planetary exploration and space satellite maintenance.

Control and motion planning with serial robots nevertheless present formidable challenges in terms of high dimensionality analysis. Numerous researchers have addressed the planning problem using different optimization strategies that have led to substantial advances [24]-[28].

To simplify the kinematics and actuation, and minimize the dynamic modeling, we suggested in previous works a minimally actuated reconfigurable track robot [29], and a preliminary design concept serial robot with a mobile actuator MASR which travels along the links to rotate the joints [30]. The MASR incorporates multiple characteristics and advantages from both minimally actuated robots and hyper redundant robots. The smaller number of motors and the simplicity of the design allow for increased reliability, smaller weight, lower costs and high modularity.

Figure 1. The minimally actuated serial robot MASR is a newly developed robot with a large number of joints and a single mobile actuator. The mobile actuator travels along the links to actuate the joints.

Here we extend on these works [29][30] and present a newer version of the MASR robot with multiple mechanical improvements which increase its strength and accuracy. The arm is now actuated vertically using a screw lead (enabling 3D motion) and the rotation of the joints is performed using worm gears which provide higher torques accuracy. The mobile actuator is now fitted with a gripper which is used to effectively translate objects along the links without having to rotate the arm. We also developed an electronic controller to automatically and more precisely control the vertical position of the arm and the translation of the mobile actuator and rotation of the links using sensors. Finally, we present a motion planner for the case in which the mobile actuator grasps objects along the arm's tip only and for the case in which the mobile actuator can carry objects along the links.

This paper is organized as follows: The design of the robot is presented in Section II. Section III deals with the kinematic analysis. Section IV focuses on developing a motion algorithm that reduces the working time and the travelled distances of the actuators. In Section V, multiple experiments performed using the robot are presented.

II. Robot design and Actuation

The MASR robot presented in this paper (Figure 2) is composed of a serial planar arm with 10 joints, a linear actuator that can displace the arm in the vertical direction and a mobile actuator that can travel along the links and rotate the joints when needed. Considerable effort was invested in keeping the design of the robot as simple as

Manuscript received: February, 2, 2020; Revised April, 23, 2020; Accepted June, 13, 2020. This paper was recommended for publication by Paolo Rocco, upon evaluation of the Associate Editor and Reviewers' comments. This research was supported By the ministry of science and technologoy and by the Helmsley Charitable Trust through the Agricultural, Biological and Cognitive Robotics Initiative and by the Marcus Endowment Fund both at Ben-Gurion University of the.

Y.Ayalon, L. Damti, and D. Zarrouk are all associated with the department of Mechanical Engineering at the Ben Gurion University of the Negev, Israel. (zadavid@bgu.ac.il).

Digital Object Identifier (DOI): see top of this page.

possible and reducing its weight. The main characteristics of the first prototype are presented in TABLE I.

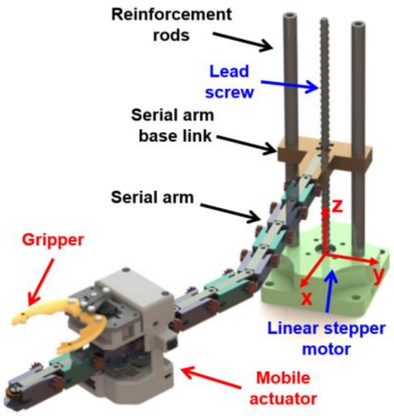

Figure 2. The mechanical design of MASR robot. The robot consists of a planar serial arm with 10 passive joints actuated by a mobile actuator. The mobile actuator that can travel over the links is fitted with a gripper to carry objects along its path. The vertical motion is actuated by a linear stepper motor.

A. Robot Design

1) The Serial Arm

The serial arm of the current design is composed of 10 identical links (Figure 3). The links are 5 cm long and 2 cm wide and are attached to each other through rotational joints. The length of the arm fitted with 10 links is 50 cm and its weight is 0.35 kg. A worm gear transmission is used to rotate the joints at a ratio of 1:38. The worm gear ensures that the links remain locked at the desired angle after the actuation is completed. The relative angle θ_j between two adjacent links (j-1 and j) can be varied in the range of [-45^o, 45^o].

At their bottom, the links have a gear rack designed to increase the traction of the mobile actuator when traveling over the links and to eliminate the possibility of sliding. In order to increase the rigidity of the 3D printed (plastic) links, aluminum supporting rods were added at their top and bottom. The weight of each link including the aluminum support is 30 grams. This 3D printed version of the robot is designed for a vertical workload of 0.5 kg. A workload of 0.5 kg causes a deformation of nearly 0.5 cm. Magnets were attached at the center of the joints to help the mobile actuator identify its location while travelling along the arm.

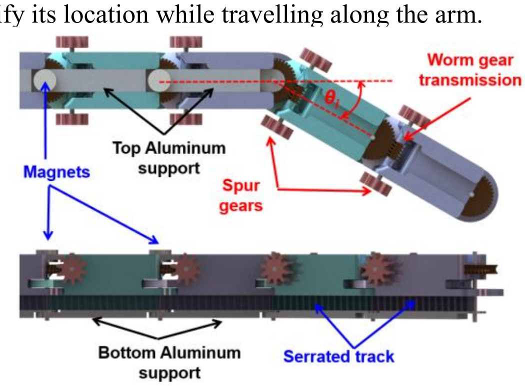

Figure 3. The robotic arm is composed of 10 links attached through rotational joints. A worm gear transmission is used to actuate the links and ensure that the relative angle is preserved when the mobile actuator departs from the joint.

2) The Mobile Actuator

The mobile actuator, presented in (Figure 4), is designed to travel over the links, stop at a designated location to rotate the joints and grasp objects using the gripper. It is composed of three separate mechanisms: the locomotive, the joint rotation mechanism and the gripper.

a) The Locomotive

The locomotive carries the actuator along the links using four serrated wheels. Two of the wheels on the one side are actuated using a rotational motor and the other two wheels, located on the other side, are passively actuated. To enable the locomotive to travel over curved joints (up to 45 degrees), the axes of the passive wheels are fixed on a rotational joint. This joint is fitted with springs, allowing the wheels to conform to the variation in the track and apply a gripping force on the tracks of the links.

b) The Joint Rotation Mechanism

The mobile actuator is fitted with a spur gear with partial gearing. When the mobile actuator reaches a specific link j, it engages the spur gear of the joint/link and rotates it. As a result, the relative angle between the two adjacent links (j and j-1) is changed (see Figure 4 and video). The partial gearing (four teeth per revolution) of the rotation mechanism is used to avoid unwanted collisions between the spur gear of the locomotive and links as the mobile actuator travels along the arm. The worm gear assembly has a ratio of 1:38, and the spur gear's ratio is 1:3, so that each full revolution of the partial spur gear will result in a 3.2 degrees rotation of the joint.

c) The Gripper

The gripper, attached to the mobile actuator, is an off-the-shelf two-finger mechanism actuated by a servo motor. It can hold objects at widths of 2.5 cm to 10.5 cm. Note that in this robot, the gripper is not fixed to the last link of the robot but rather to the mobile actuator. As a result, the mobile actuator can travel over the links to grasp objects and translate them along the arm. More sophisticated grippers with more fingers can be attached to the mobile actuator if needed. The gripper can also be replaced with a welding tool, a saw, or a paint brush for example, depending on the application requirements.

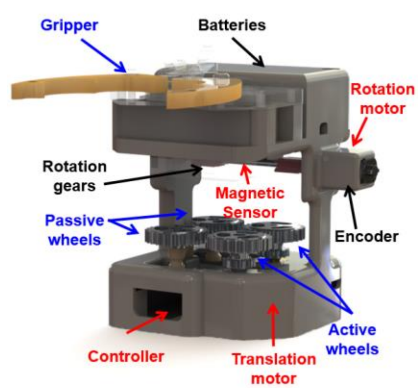

Figure 4. The mobile actuator is composed of a locomotive mechanism, a rotation mechanism and a gripper. The mobile actuator holds its controller and batteries onboard.

3) The Vertical Driving Mechanism

Vertical motion (z direction) is enabled by a lead screw rotated with a stepper motor located at the base of the robot. The diameter of the screw is 8 mm and its pitch 8 mm. Because the stepper motor makes 200 steps per revolution, the nominal accuracy of the motion is 0.04 mm. To reinforce the structure to prevent bending, two 10 mm steel rods are attached to the base of the robot (Figure 2). The total range of the vertical motion is 38 cm.

4) Manufacturing

The robot is mostly manufactured from 3D printed materials. The links, which require high resolution, were printed using a Polyjet printer (Object Connex 350) and the mobile actuator was printed using an FDM printer. To increase the strength of the serial arm and minimize bending, 3 mm thick aluminum rods were attached on the top and bottom of the links. Since there is no wiring along the links, their replacement is very simple.

TABLE I. CHARACTERISTIC PARAMETERS OF THE ROBOT.

Serial arm Length (10 links)		50 cm
Serial arm weight (10 links)		0.35 kg
Mobile actuator weight		0.3 kg
Joint rotation speed		15 degrees/s
Mobile actuator speed		12.5 cm/s
Vertical speed		10 cm/s
Vertical workload		0.5 kg
Side forces		0.1 kg
Precision		0.5 cm

B. Actuation and Control

1) Actuation

The MASR robot, including its gripper, is actuated using a total of four motors:

- One 12 V stepper motor to move the arm in the vertical direction. The stepper motor produces a torque of 36 Ncm. For the given lead screw diameter and pitch (both 8 mm) and assuming that the coefficient of friction is 0.3, the motor and lead screw setup can produce an estimated vertical force of 140 N [31].
- Two DC motors: one motor to drive the mobile actuator along the links, and the other motor to rotate the joints of the links. Both motors are 12 mm in diameter (6-9 Volts manufactured by Pololu), which can be purchased at different gear ratios and can be fitted with magnetic encoders.
- An off-the shelf servo motor to actuate the gripper.

2) Control

The robot is controlled by two electronic control boards that are synchronized using RF module communication. The mobile actuator is controlled with a Teensy 3.5 controller (compatible with Arduino software) that controls its locomotion, its rotational mechanism and its gripper. The angular displacement of the rotational mechanism is measured using a magnetic encoder fitted to the motor's shaft and yields 12 counts per motor revolution. The motors are powered by two 3.7 Volts 800 mAh LiPo batteries connected in series.

To ensure that the mobile actuator stops accurately at the precise location to engage the gears of the links and rotate the joints, tiny magnets were inserted in the centers of the joints and a magnetic Hall effect sensor (A1302) was attached to the mobile actuator. The stepper motor that actuates the vertical motion is controlled with an Arduino Uno board. The two controllers communicate via a NRF24L01 Radio Transceiver Module that transmits and receives commands and other data such as location and orientation between the two controllers.

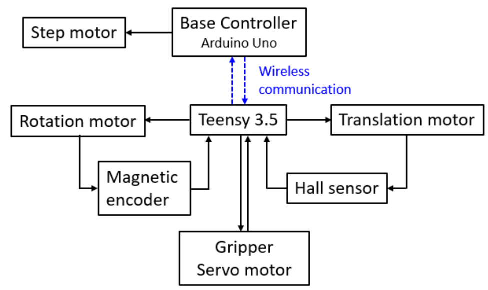

Figure 5. The electronic control system of the robot.

III. KINEMATIC MODEL

We assume that our robot is composed of N identical links (not including the base link) whose length is L, connected using N rotational joints. Since the manipulator is confined to the horizontal plane (x,y) and the linear screw to the vertical direction (z), the motion of the two mechanisms can be decoupled and the analysis can be performed separately.

1) Position and Speed

The links are numbered from 0 (the base link) to N which represents the last link in the serial arm. The joint angle j between the links j-1 and j is denoted by θ_j, and the relative orientation of link j to the base link by α_j. The position of joint j (x_j, y_j, z) of the robot and its orientation α_j are given by:

$$\mathbf{X_j} = \begin{bmatrix} x_j \\ y_j \\ z \\ \alpha_j \end{bmatrix} = \begin{bmatrix} L\sum_{m=1}^{j}\cos\left(\sum_{m=1}^{n}\theta_m\right) \\ L\sum_{n=1}^{j}\sin\left(\sum_{m=1}^{n}\theta_m\right) \\ z_j \\ \sum_{m=1}^{j}\theta_m \end{bmatrix} \quad (1).$$

The mobile actuator in our robot can either travel along the links or rotate the joints. Therefore, the speed $\dot{\mathbf{X}}_\mathbf{j}$ of a joint j can be calculated using the Jacobian matrix $\mathbf{J_j}$ like other regular serial robots:

$$\dot{\mathbf{X}}_\mathbf{j} = \mathbf{J_j}\begin{bmatrix} \dot{\boldsymbol{\theta}} \\ \dot{z} \end{bmatrix} \quad (2).$$

where the Jacobian matrix is defined as:

$$\mathbf{J_j} = \left[\frac{\partial X}{\partial\theta_1}\cdots\frac{\partial X}{\partial\theta_j},\frac{\partial X}{\partial z}\right] \quad (3).$$

Note that since a single mobile actuator is currently being used, the different joints of the serial arm can be actuated one at a time. The total time required to reconfigure the angles of the joints and reach a specific target is composed of the time required to travel along the links, to engage the joints, rotate them and disengage from them. The vertical motion along the vertical direction can be performed in parallel to the motion of the serial arm.

If we assume a constant lifting and lowering velocity V_z of the vertical motor and constant linear and rotational speeds of the mobile actuator, respectively V_m and ω, the time required to reach a target is:

$$\Delta T = \mathrm{Max}\left(\frac{1}{\omega}\sum_{1}^{N}\left|\Delta\theta_j\right| + \frac{d_T}{V_m} + n\cdot T_{\mathrm{STOP}}\,;\,\frac{\Delta z}{V_z}\right) \quad (4)$$

where $\Delta\theta_j$ the is rotation of joint j, d_T is the total distance travelled by the mobile actuator, n is the number of rotated joints and T_{STOP} is the time required to start and stop the mobile actuator.

2) *Workspace*

Given that the joints in the current design are limited to rotating by a maximum of 45 degrees to either side, we determined the work volume of the serial arm in the 2D space as a function of the number of links. The work volume was determined by exhaustively searching the total space for possible solutions (not including orientation), using the motion planning algorithm presented in Section IV. At six links, the arm can already reach areas behind its base. The size of the work area (2D space) continues to increase with the number of links. The size of the workspace is nearly four times larger with 10 links compared to its size with 6 links. The size of the workspace as a function of the links is presented in TABLE II.

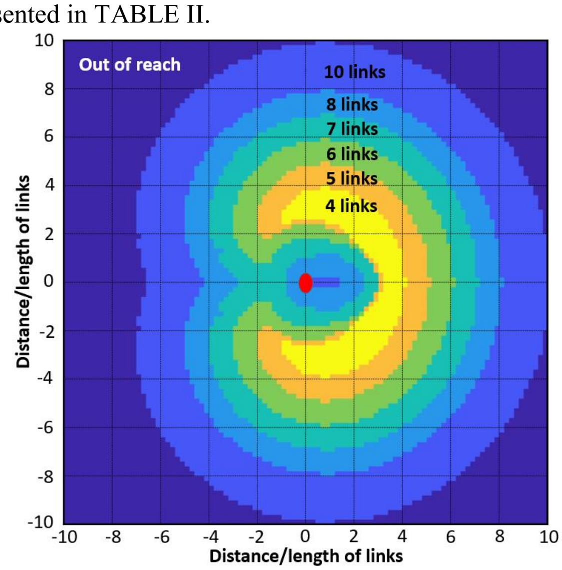

Figure 6. Top view of the work volume of the robot as a function of the number of links.

TABLE II. SIZE OF THE WORKSPACE AS A FUNCTION OF N.

No. of links N	4	5	6	7	8	10
Work space $[L^2]$	8.3	18.9	35.8	58.7	83.5	136.7

where L is the length of a single link.

IV. 2D MOTION PLANNING ALGORITHM

The MASR robot is a minimally actuated overly redundant robot; i.e., there is an infinite number of solutions to reach a specific point in the plane using the robotic arm. Our aim in this planning algorithm is to reduce the location error, the travelling distance of the mobile actuator, its number of stops to rotate the joints and the total time required to perform a task. Assuming an obstacle-free space, and that the arm's initial configuration is $\boldsymbol{\theta}\mathbf{i}$, (initial position and orientation $\mathbf{Xi}$=(x_i,y_i,α_i)), the goal is to determine the joint rotation $\Delta\boldsymbol{\theta}_\mathbf{j}$ which will lead the arm to the final location $\mathbf{Xf}$=(x_f,y_f,α_f).

Our algorithm is based on minimizing a cost function F($\Delta\boldsymbol{\theta}_\mathbf{j}$, $\boldsymbol{\theta}\mathbf{i}$, $\mathbf{X_f}$) which combines the original orientation of the links, the proximity of the robot to the target point and the variation of the joint angles from the original to the final configuration. We minimized the function using Matlab's *fmincon* function which can find a *local minimum* within given upper and lower bounds (such as the minimum and maximum values of the rotation angle, negative 45 degrees to positive 45 degrees). To increase its chances of finding the global minimum and improve the results, we ran the function 100 times with different randomly chosen original solution guesses and the solution with the lowest cost function was chosen. Throughout this analysis, we assumed that the robot was composed of 10 identical links whose length L is 5 cm (similar to the experimental robot). In the following examples, solutions were accepted only if the maximum distance from the target was less than 0.2 cm and the orientation error of the last link was less than 0.5 degrees.

A. *Reaching a Target with the Tip of the Last Link (**LL**)*

Although the mobile actuator carries the gripper, in many applications grasping an object may be possible only if the gripper is located on the last link of the serial arm. In this case, the tip of the robot must reach the desired location and the last link must have the same orientation as the target. The cost function F is composed of the three functions, f_{TIP} and f_{OR} which respectively weigh the distance and orientation of the last link from the target and the function f_{STOPS} which weighs the number of the actuated joints.

$$F\left(\Delta\boldsymbol{\theta}_\mathbf{j},\boldsymbol{\theta}_\mathbf{i},\mathbf{X_f}\right) = w_1 f_{\mathrm{TIP}} + w_2 f_{\mathrm{OR}} + w_3 f_{\mathrm{STOPS}} \quad (5).$$

The proximity function f_{TIP} is simply defined as the norm of the vector error of the tip of the robot from the target point:

$$f_{\mathrm{TIP}} = \mathrm{norm}\left(\mathbf{X_F} - \mathbf{X_N}\right) \quad (6).$$

The orientation function f_{OR} is the square of the difference between the orientation of the last joint to the orientation of the tip of the robot:

$$f_{\mathrm{OR}} = \left(\alpha_N - \alpha_T\right)^2 \quad (7).$$

The function f_{STOPS} is negative and sums the values of the changes in the joints at the power n.

$$f_{\mathrm{STOPS}} = -\sum_{j=1}^{N}\left|\Delta\theta_j^n\right| \quad (8).$$

If the power n is larger than 1, the algorithm attempts to increase the variation of the joints. Given that the sum of the variation is limited by the orientation of the last link, the algorithm attempts to reduce the number of active joints and increase their rotation. In the solution we used identical weights $w_1=w_3=1$ whereas $w_2=200$ in order to increase its influence. The value of $w_2 * f_{OR}$ is equal to one if the error is nearly 0.2 degrees (0.0035 Radians).

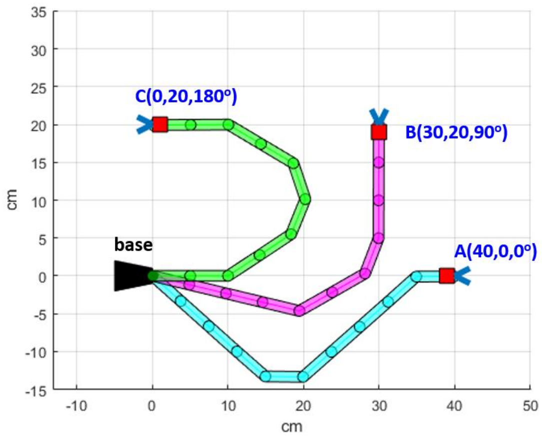

Figure 7. Starting from an initial configuration where all the joints were at 0 degrees, the robot reaches points A, B, and C using the LL method.

TABLE III. SOLUTION FOR A,B, AND C USING THE "LL" METHOD.

Joint No.	Initial config.	Point A (40,0,0°)	Point B (30,20,90°)	Point C (0,20,180°)
1	0	-41.8	-13.4	0
2	0	0	0	0
3	0	0	0	33.2
4	0	0	0	0
5	0	0	43	34.1
6	0	41.6	0	40.7
7	0	42	39.2	40.7
8	0	0	20.9	0
9	0	0	0	31.1
10	0	-41.4	0	0
Active joints	-	4	4	5
Δd [cm]	-	0.07	0.13	0.07
Δθ [deg]	-	-0.29	0.07	0.38
Travelled d.	-	50 cm	50 cm	50 cm
rotation		167°	117°	180°
Conv. rate		69%	75%	84%

In the following example (Figure 7), we searched for a solution to three different target points with given orientations $\mathbf{X_A}(40,0,0°)$, $\mathbf{X_B}(30,20,90°)$, and $\mathbf{X_C}(0,20,180°)$. Starting from an initial configuration where the mobile actuator was at the origin and all the joint angles were 0°, the algorithm success rate in finding a solution within the accepted range (position error < 0.2 cm and orientation error < 0.5 degrees) was 69% in A, 75% in B, and 84% in C. For point A, a solution was found by rotating only four joints and the errors were 0.07 cm and -0.29 degrees. In B, a solution was found by rotating only four joints and the error is 0.13 cm and 0.07 degrees. In C, five joints were rotated, and the error was 0.07 cm and 0.38 degrees. For each point, one of the results with the smallest number of actuated joints is presented in TABLE III. The average success rate of the algorithm in finding a solution in the whole workspace for 10 links which includes 3342 points (as per Figure 6) is 92.4 % while the average running time per solution is 1.5 seconds. Note that since the joints are limited to rotate in the range of ±45 degrees only, a collision can occur if seven consecutive joints are rotated by +45° or if seven consecutive joints are rotated by -45°. In such a case, a different solution must be sought using different initial values.

This algorithm is efficient if the rotation angle range is relatively small such as in our case. If larger rotation angles were allowed, a function reducing the total sum of joint rotations must be added to the cost function in order to avoid the collapse of the links on each other.

*B. Reaching a Target with Any Link (**AL**)*

One of the unique features of the MASR robot is that its gripper can reach a specific target if any of the links is above or below the target (see Figure 9 and video). This feature is especially useful if the target point is close to the base link or if the mobile actuator is required to move objects along the path of the links. If the target point is above or below a given link j, the distance from the line along (collinear) the link j to the target, denoted by d_{LINK}, must be zero. The target point must also be within the boundaries of the link; i.e., between joint j and j+1 (see Figure 8). We denote the distance between the target to adjacent joints by d_j and d_{j+1}. In order to satisfy this condition, both distances must be simultaneously smaller than the length of the link L.

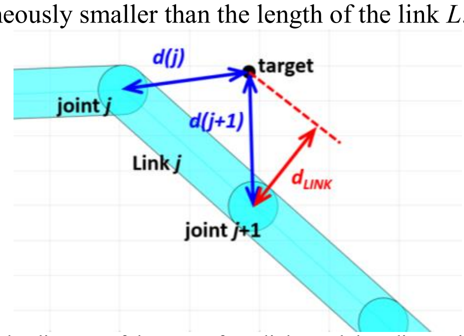

Figure 8. The distance of the target from link j and the adjacent joints (j and j+1).

The cost function in the *AL* case is defined as:

$$F\left(\boldsymbol{\Delta\theta_j}, \boldsymbol{\theta_i}, \mathbf{X_f}\right) = w_1 f_{\text{LINK}} + w_2 f_{\text{OR}} + w_3 f_{\text{STOPS}} \quad (9).$$

where f_{OR} and f_{STOPS} and the weights w_i are identical to the *LL* case, and f_{LINK} is defined as:

$$f_{\text{LINK}} = d_{\text{LINK}}{}^2 + f_{\text{JOINT}}\left(j\right) + f_{\text{JOINT}}\left(j+1\right) \quad (10)$$

and the function f_{JOINT} is:

$$f_{\text{JOINT}}\left(j\right) = \text{abs}\left(L - d\left(j\right)\right) - \left(L - d\left(j\right)\right) \quad (11).$$

The cost function $f_{\text{JOINT}}(j)$ becomes zero if the distance between the joint to the target point is less than L and positive (linearly monotonous) if the distance is larger than L. Minimizing the combination of $f_{\text{JOINT}}(j)$, $f_{\text{JOINT}}(j+1)$, together with the distance d_{LINK} ensures that the target point is on the link j.

The results of the algorithm that found an optimal solution for the three points A,B and C (points identical to the previous section), are presented in Figure 1 and summarized in TABLE IV. The algorithm successfully found solutions at high convergence rates (respectively 96%, 84% and 98% for A, B and C). The solution for A is trivial and the mobile actuator travelled a distance of 40 cm along the links without rotating any joint. In B, the mobile actuator rotated only 3 joints and reached the point using its 9th link after travelling 45 cm. In C, the rotation of 5 joints was required and the robot reached the point with its 6th link.

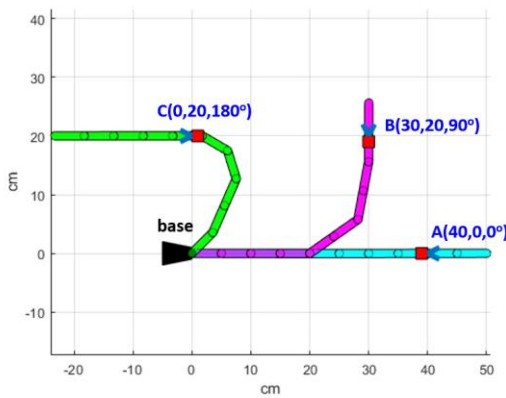

Figure 9. Starting at an initial configuration where all the joints were at 0 degrees, the robot reached points A, B, and C using the AL method.

TABLE IV. SOLUTION FOR A, B, AND C USING THE "AL" METHOD.

Joint No.	Initial config.	Point A (40,0,0º)	Point B (30,20,90º)	Point C (0,20,180º)
1	0	0.0	0.0	45.0
2	0	0.0	0.0	21.5
3	0	0.0	0.0	0
4	0	0.0	0.0	40.7
5	0	0.0	35.2	42.4
6	0	0.0	0.0	30.4
7	0	0.0	44.2	0
8	0	0.0	0.0	0
9	0	0.0	10.2	0
10	0	0.0	0.0	0
Active joints	-	0	3	5
Δd [cm]	-	0.00	0.004	0.006
Δθ [deg]	-	0.00	0.23	0.03
Travelled d.	-	40 cm	45 cm	30 cm
Rotation		0 º	90 º	180º
Conv. Rate		96%	84%	98%

C. Comparing the LL and the AL Methods

In this section, we compare the distance travelled by the mobile actuator, the total angular rotation of the joints, the number of stops and the total time. Using Eq. (4) and assuming that V_m =20 cm/s and ω=360 degrees/s and that T_{STOP}=0.1 s, the total time required for performing the mission can be calculated. A comparison between the two methods is presented in TABLE V. The results show that the AL method is substantially faster than LL (by 20% to 45%).

TABLE V. COMPARING THE METHODS REACHING POINTS A, B AND C

	Point A	Point B	Point C
Distance LL	45	45	45
Distance AL	40	45	25
Angular LL [deg.]	167	116	180
Angular AL [deg.]	0	90	180
Stops LL	5	6	7
stops AL	1	3	5
Total time LL [s]	3.7	3.5	4
Total time AL [s]	2.1	3	2.7

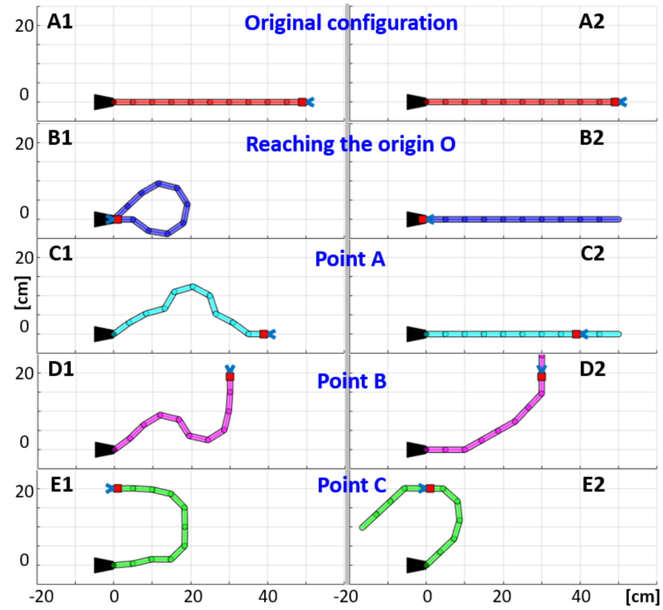

Figure 10. Comparison of the LL and AL methods performing consecutive tasks. Starting from its original configuration, the robot moves its mobile actuator to points O, A, B and C.

Next, we compared the two methods when performing consecutive tasks by travelling to the origin O and then to points A, B and C. The results of the comparison are presented in Figure 10 and table VI.

TABLE VI. COMPARING THE METHODS WHEN TRAVELLING ALONG THE PATH OABC

	O	OA	AB	BC	OABC
Distance LL [cm]	45	90	90	90	315
Distance AL [cm]	0	40	45	75	160
Angular LL [º]	339	209	333	266	1147
Angular AL[º]	0	0	90	133	223
Stops LL	8	5	7	7	27
stops AL	0	1	4	5	10
Total time AL [s]	4.9	6.2	7.1	6.7	24.8
Total time L[s]	0	2.1	3.1	5	10.3

Starting from the original configuration "A1", the robot in the LL case must rotate 9 of its joints to reach the origin "B1", whereas in the AL method it does not rotate any joints at all "B2". The same holds in case "C" as in the AL method, where the mobile actuator only needs to travel to link 8 without rotating any of its joints. In case "D2", using the AL method, the target can be reached by only using 9 links and in "E2" by only using 6 links. TABLE VI. presents the number of steps required and time elapsed for task performance. It shows that performing the task using the AL method is substantially faster (nearly 60%) and reduces the distance travelled by the mobile actuator and rotated joints.

V. EXPERIMENTS AND RESULTS

This section presents the results of the experiments conducted with a 3D printed prototype of the robot. We tested its full functionality in multiple experiments which included reaching different points in 3D space, picking up objects with the mobile actuator, translating them using the mobile actuator while travelling over the links and releasing them at the target points. The experiments were pre-planned offline using our optimization algorithm and performed automatically using the robot (see video).

A. Translating an Object Located Above the Links

The first experiment using this robot mimicked picking a piece of fruit from a tree and placing it in a basket. Starting at A, the vertical actuator raises the arm by 26 cm while the mobile actuator advances slightly towards the ball "B" hanging from the top with a nylon wire. The mobile actuator grasps the ball in "C" and advances to the 5^{th} joint while rotating it by 4 degrees "D". Then, the mobile actuator advances to the 6^{th} joint while rotating it by 24 degrees "E" and continues towards the 10^{th} link to drop the ball into the target bowl "F". See attached video.

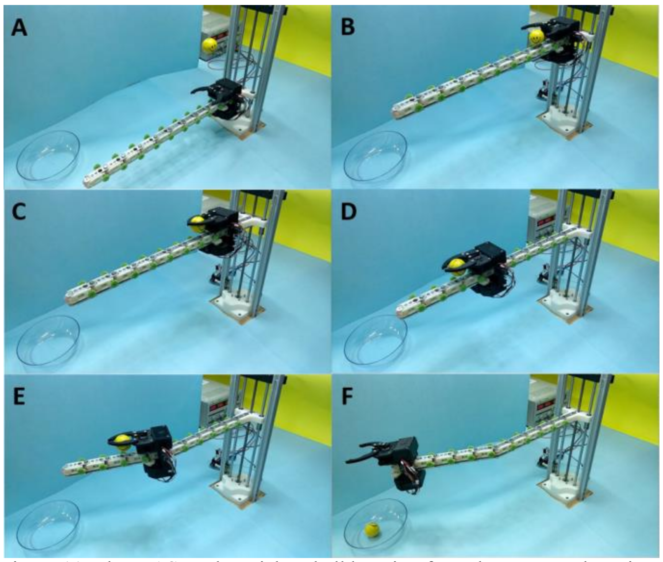

Figure 11. The MASR robot picks a ball hanging from the top, translates it along the links and drops it into a basket.

B. Relocating an Object

In this experiment, the robot's task was to move the position of a cup using a minimal number of joints. The origin and target locations of the cup were at different heights. Starting in "A", the linear vertical actuator raises the arm by 10 cm. Moving forward, the mobile actuator advances to the 7^{th} and the 8^{th} joints and rotates their angles by 28 and 16 degrees respectively "B". Then, the mobile actuator continues advancing along the links to reach cup "C". After grasping the cup, the linear vertical actuator raises the arm by 12 cm, while the mobile actuator returns to the 8^{th} link "D" and rotates it into negative 16 degrees and the 7^{th} link into negative 28 degrees "E". The mobile actuator then moves along the links and places the cup in the target location "F". See attached video.

C. Reaching Around an Obstacle

In the last experiment presented here, the mobile actuator rotated the links to go around an obstacle (simulating a wall) to reach the target. The wall was 7 cm away in the y direction from the origin of the robot and was 25 cm long (from x= 0 to x=25 cm). The target location was (10, -20). Starting from straight configuration "A", the mobile actuator travels toward the 8^{th} joint ("B" to "D") and rotates the joints [(5, -38 ^{o}) (6, -39 ^{o}) (7, -38 ^{o}) (8, -35 ^{o})] as it advances. Then the mobile actuator proceeds to the last link "E" and releases the ball "F". See attached video.

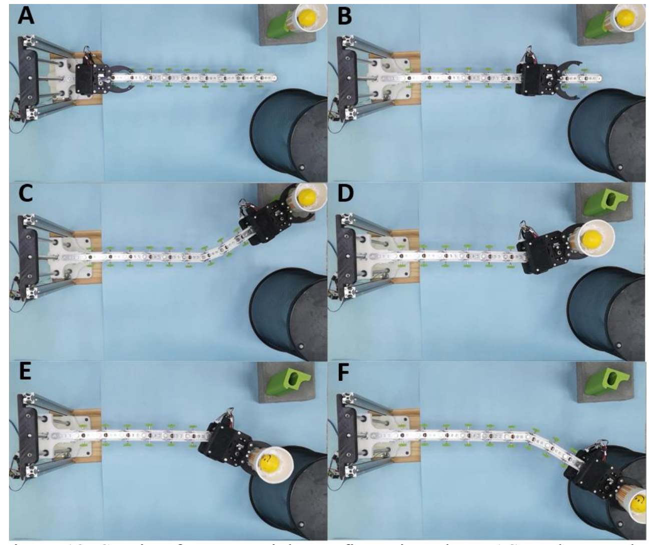

Figure 12. Starting from a straight configuration, the MASR relocates the of the cup.

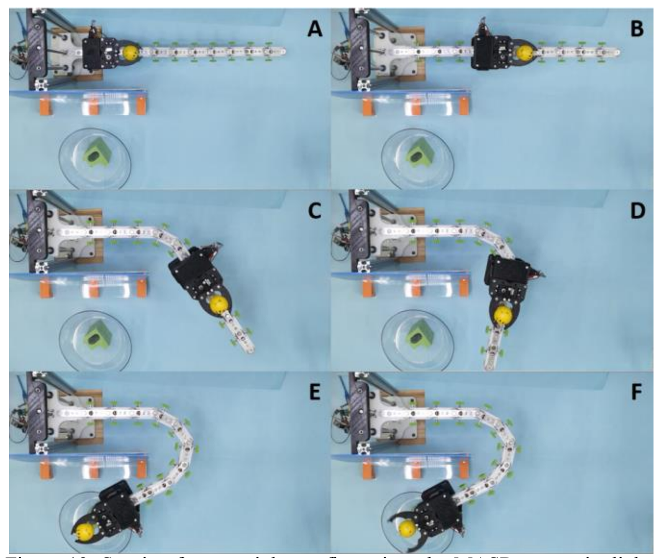

Figure 13. Starting from straight configuration, the MASR rotates its links to turn around an obstacle.

VI. CONCLUSIONS

In this paper, we presented a novel serial robot composed of a multi linkage arm with passive joints and a mobile actuator that can travel along the arm and rotate the links. The mobile actuator is fitted with a gripper that allows it to grasp objects along its path and translate them quickly along the arm. This design makes it possible to reduce the size of the robot, its weight and simplify its design. As it has no wiring along the links, the links can be easily replaced and their size and number simply changed according to the requirement of the task. The mobile actuator can also be replaced, and more than one mobile actuator can be used.

We developed a locomotion algorithm based on optimizing a time-based function to minimize the operation time and actuation of the robot. Since our gripper can be moved along the links, we compared the time requirements for a task in which the robot relocates an object from one point to another with a given orientation for two situations: 1) the gripper can only grasp an object when the gripper is at the last link "LL". 2) The gripper can grasp objects at any link along the arm "AL". A comparison of the time elapsed in each of the two methods shows that in the second case, the time can be reduced by nearly three-fold.

Finally, we developed an experimental prototype of the robot which can automatically perform its pre-planned tasks. We used the robot to demonstrate multiple tasks which include relocating objects by rotating a minimal number of joints and translating objects along the robot's arm. The 3D printed version with aluminum reinforcement is designed for a workload 0.5 kg which can cause a deformation of up to 0.5 cm at its tip due to the flexibility of the links and the backlash of the joints. Decreasing the number of links will decrease the deformation and vice versa.

Note that while this robot is very simple and lightweight, it is substantially slower than regular fully actuated serial arms. Therefore, this robot should be used in applications where high speed is not required such as space applications, agriculture, maintenance, painting and search and rescue operations, for example.

Our future work will focus on using multiple mobile actuator, improving the design and developing a metal version to reduce the deformation. We also plan to study the mobility of the MASR in 3D space and developing more advanced motion planning algorithms.

VII. REFERENCES

[1] K. Ning, and F. WÖrgÖtter, "A Novel Concept for Building a Hyper-Redundant Chain Robot," *IEEE Transactions on Robotics*, vol. 25, no. 6, pp. 1237-1248, 2009.

[2] P. Schrock, F. Farelo, R. Alqasemi, and R. Dubey, "Design, simulation and testing of a new modular wheelchair mounted robotic arm to perform activities of daily living," IEEE International Conference on Rehabilitation Robotics, Kyoto, pp. 518-523, 2009.

[3] E. Shammas, A. Wolf, H. B. Brown, and H. Choset, "New joint design for three-dimensional hyper redundant robots," IEEE/RSJ International Conference on Intelligent Robots and Systems, Las Vegas, NV, USA, vol. 3, pp. 3594-3599, 2003.

[4] A. Wolf, H. B. Brown, R. Casciola, A. Costa, M. Schwerin, E. Shamas, and H. Choset , "A mobile hyper redundant mechanism for search and rescue tasks," IEEE/RSJ International Conference on Intelligent Robots and Systems, Las Vegas, NV, USA, vol. 3, pp. 2889-2895, 2003.

[5] I. Erkmen, A. M. Erkmen, F. Matsuno, R. Chatterjee, and T. Kamegawa, "Snake robots to the rescue!" *IEEE Robotics & Automation Magazine*, vol. 9, no. 3, pp. 17-25, 2002.

[6] H. Maruyama, and K. Ito, "Semi-autonomous snake-like robot for search and rescue," IEEE Safety Security and Rescue Robotics, Bremen, pp. 1-6, 2010.

[7] T. Kamegawa, T. Yarnasaki, H. Igarashi, and F. Matsuno, "Development of the snake-like rescue robot "kohga"," IEEE International Conference on Robotics and Automation, New Orleans, LA, USA, vol. 5, pp. 5081-5086, 2004.

[8] J. Borenstein, M. Hansen, and A. Borrell, "The OmniTread OT-4 Serpentine Robot 1 – Design and Performance," *Journal of Field Robotics*, vol. 24, pp. 601-621, 2007.

[9] M. Arai, Y. Tanaka, S. Hirose, H. Kuwahara, and S. Tsukui, "Development of "Souryu-IV" and "Souryu-V": Serially connected crawler vehicles for in-rubble searching operations," *Journal of Field Robotics*, vol. 25, pp. 31-65, 2008.

[10] K. Suzuki, A. Nakano, G. Endo, and S. Hirose, "Development of multi-wheeled snake-like rescue robots with active elastic trunk," IEEE/RSJ International Conference on Intelligent Robots and Systems, Vilamoura, pp. 4602-4607, 2012.

[11] H. Komura, H. Yamada, and S. Hirose, "Development of snake-like robot ACM-R8 with large and mono-tread wheel," *Advanced Robotics*, vol. 29, pp. 1081-1091, 2015.

[12] K. Ito, and M. Haruo. "Semi-autonomous serially connected multi-crawler robot for search and rescue," *Advanced Robotics*, vol. 30, no. 7, pp. 489-503, 2016.

[13] T. Ota, A. Degani, D. Schwartzman, B. Zubiate, J. McGarvey, H. Choset and M. A. Zenati, "A Highly Articulated Robotic Surgical System for Minimally Invasive Surgery," The Annals of Thoracic Surgery, vol. 87, pp. 1253-1256, 2009.

[14] A. Degani, H. Choset, A. Wolf and M. A. Zenati, "Highly articulated robotic probe for minimally invasive surgery," IEEE International Conference on Robotics and Automation, Orlando, FL, pp. 4167-4172, 2006.

[15] K. Ikuta, T. Hasegawa and S. Daifu, "Hyper redundant miniature manipulator "Hyper Finger" for remote minimally invasive surgery in deep area," IEEE International Conference on Robotics and Automation, Taipei, Taiwan, vol. 1, pp. 1098-1102, 2003.

[16] N. Simaan, R. Taylor and P. Flint, "A dexterous system for laryngeal surgery," IEEE International Conference on Robotics and Automation, New Orleans, LA, USA, vol. 1, pp. 351-357, 2004.

[17] J. Burgner-Kahrs, D. C. Rucker and H. Choset, "Continuum Robots for Medical Applications: A Survey," IEEE Transactions on Robotics, vol. 31, no. 6, pp. 1261-1280, 2015.

[18] R. J. Webster, A. M. Okamura and N. J. Cowan, "Toward Active Cannulas: Miniature Snake-Like Surgical Robots," IEEE/RSJ International Conference on Intelligent Robots and Systems, Beijing, pp. 2857-2863, 2006.

[19] Z. Mu, T. Liu, W. Xu, Y. Lou, and B. Liang, "Dynamic feedforward control of spatial cable-driven hyper-redundant manipulators for on-orbit servicing," *Robotica*, vol. 37, no. 1, pp. 18–38, 2019.

[20] V. A. Sujan, M. D. Lichter, and S. Dubowsky, "Lightweight hyper-redundant binary elements for planetary exploration robots," IEEE/ASME International Conference on Advanced Intelligent Mechatronics, Como, Italy, vol. 2, pp. 1273-1278, 2001.

[21] M. Yim, K. Roufas, D. Duff, Y. Zhang, C. Eldershaw, and S. Homans, "Modular Reconfigurable Robots in Space Applications," *Autonomous Robots*, vol. 14, pp. 225–237, 2003.

[22] C. Fan, Y. Zhang, Z. Xie, Y. Liu, Z. Li, C. Li, and H. Liu, "Design of Space Robotic Arm-Hand System and Operation Research," IEEE International Conference on Mechatronics and Automation, Changchun, pp. 481-486, 2018.

[23] I. D. Walker, "Robot strings: Long, thin continuum robots," IEEE Aerospace Conference, Big Sky, MT, USA, pp. 1-12, 2013.

[24] L. Pfotzer, S. Klemm, A. Rönnau, J. M. Zöllner, and R. Dillmann, "Autonomous navigation for reconfigurable snake-like robots in challenging, unknown environments," *Robotics and Autonomous Systems*, vol. 89, pp. 123-135, 2017.

[25] M. S. Menon, V. C. Ravi, and A. Ghosal, "Trajectory Planning and Obstacle Avoidance for Hyper-Redundant Serial Robots," *ASME. J. Mechanisms Robotics*, vol. 9, no. 041010-1, 2017.

[26] E. K. Xidias, "Time-optimal trajectory planning for hyper-redundant manipulators in 3D workspaces," *Robotics and Computer-Integrated Manufacturing*, vol. 50, pp. 286-298, 2018.

[27] J. Zhao, L. Zhao, and Y. Wang, "A Novel Method for the Motion Planning of Hyper-redundant Manipulators Based on Monte Carlo," *Mechanism and Machine Science*, vol. 408, pp. 11-22, 2017.

[28] A. Motahari, H. Zohoor, and M. H. Korayem, "A new motion planning method for discretely actuated hyper-redundant manipulators," *Robotica*, vol. 35, no. 1, pp. 101–118, 2017.

[29] M. P. Mann, L. Damti, G. Tirosh, and D. Zarrouk, "Minimally actuated serial robot", *Robotica*, vol. 36, no. 3, pp. 408–426, 2018.

[30] T. Kislassi, and D. Zarrouk, "A Minimally Actuated Reconfigurable Continuous Track Robot," *IEEE Robotics and Automation Letters*, doi: 10.1109/LRA.2019.2959237, 2019.

[31] R. L Norton, "Machine design, an integrated approach", (Pearson, Edition 5), 2013.